Scientific Research Publishing

Journal of Biosciences and Medicines, 2022, 10, 82-99
https://www.scirp.org/journal/jbm
ISSN Online: 2327-509X
ISSN Print: 2327-5081

Construction and Analysis of an Immune-Related Gene Prognostic Index for Bladder Cancer

Chen Gong, Qi Zhao, Hao Huang, Xiaowu Pi, Feng Guo, Jun Li, Ying Xiong*

The First Affiliated Hospital of Yangtze University, Jingzhou, China
Email: *31350266@qq.com

How to cite this paper: Gong, C., Zhao, Q., Huang, H., Pi, X.W., Guo, F., Li, J. and Xiong, Y. (2022) Construction and Analysis of an Immune-Related Gene Prognostic Index for Bladder Cancer. *Journal of Biosciences and Medicines*, **10**, 82-99.
https://doi.org/10.4236/jbm.2022.108008

Received: July 6, 2022
Accepted: August 7, 2022
Published: August 10, 2022

Abstract

Objective: To construct an Immune-Related Gene Prognostic Index (IRGPI) for bladder cancer using a bioanalytical approach to analyze its molecular and immunological characteristics, as well as to assess the benefit of Immune Checkpoint Inhibitor (ICI) therapy in the IRGPI-defined bladder cancer subgroup. **Methods:** Twenty-nine immune-related pivotal genes were identified by Weighted Gene Co-expression Network Analysis (WGCNA) based on The Cancer Genome Atlas (TCGA) bladder cancer immune dataset (n = 433). Six genes were identified using a multifactorial Cox regression approach to construct the IRGPI and validated against the Gene Expression Omnibus (GEO) dataset (n = 256). Then, molecular and immunological features in the subgroups defined by IRGPI were synthesized by GSEA, Kaplan-Meier survival curves, and other methods, and the benefit of ICI treatment was assessed. **Results:** IRGPI was constructed based on six genes including AHNAK, ILK, OGN, PDGFD, PPARGC1B, and JAM3. Patients with low IRGPI had better Overall Survival (OS) than those with high IRGPI, which was confirmed in the validation cohort of GEO. Pooled analysis showed that the low IRGPI subgroup was associated with higher infiltration of CD8 T cells, activated memory CD4 T cells, and could benefit from ICI treatment. Meanwhile, high IRGPI subgroups were associated with higher resting memory CD4T cells, M0 macrophages, and M2 macrophage content, immunosuppression, and benefited less from ICI treatment. **Conclusion:** IRGPI is a novel biomarker with better efficacy in differentiating the prognosis of bladder cancer, molecular and immune features, and evaluation of ICI therapy for individualized treatment of bladder cancer.

Keywords

Bladder Cancer, Immune-Related Genes, IRGPI, Survival Prognosis

*Corresponding author.

1. Introduction

Bladder cancer is a common malignant tumor with the highest incidence and mortality rate among urological tumors [1] [2]. The traditional treatment of solid tumors is mainly surgical resection and chemotherapy [3] [4], but with the rise of immunotherapy, immune checkpoint inhibitors represented by PD-1 and PD-L1 have achieved very good therapeutic results in tumor treatment [5] [6].

The advent of immunotherapy has fundamentally changed the oncology treatment strategy, giving hope to some oncology patients, especially those with advanced cancer who are not sensitive to chemotherapy [7] [8]. Immunotherapy may be a better option for a small group of patients with bladder cancer [9]. Several biomarkers are available to help us better tap into these potentially beneficial patients, but their credibility needs to be validated. Clinical limitations similar to TMB and PD-L1 still exist in predicting tumor immunosuppressive site therapy [10] [11]. Also, there is limited research on the immune microenvironment (TME) of bladder cancer [12]. Therefore, establishing validated prognostic and therapeutic indicators is important for clinical decision-makers in the choice of diagnosis and treatment.

In this study, we used bladder cancer data from The Cancer Genome Atlas (TCGA) project to analyze differentially expressed genes in bladder cancer samples and normal samples, obtained immune-related differentially expressed genes after comparing them with immune-related genes in ImmPort, and screened them by Weighted Gene Co-expression Network Analysis (WGCNA) for prognosis The immune pivotal genes directly related to prognosis were screened by Weighted Gene Co-expression Network Analysis (WGCNA), and then a new validated Immune-Related Gene Prognostic Index (IRGPI) identifying bladder cancer mortality risk was constructed. Meanwhile, the molecular and immune characteristics of the constructed IRGPI were analyzed to determine its prognostic role in immunotherapy, and then compared with other tumor biomarkers, such as TIDE and TIS. Overall, IRGPI is a promising prognostic biomarker.

2. Methods

2.1. Patients and Datasets

Clinical characteristics, RNA-seq expression data, and somatic mutation information of bladder cancer patients were collected from the Tumor Genome Atlas database (https://portal.gdc.cancer.gov/). A total of 433 samples of RNA-seq expression data were collected, including 19 normal samples and 414 tumor samples. RNA sequence data and survival information of 256 bladder cancer samples (GSE13507) were downloaded from the GEO database (https://www.ncbi.nlm.nih.gov/geo/). The list of immune-associated genes was obtained from ImmPort (https://www.immport.org/shared/home).

2.2. Identification of Immune-Related Core Genes

A list of differentially expressed genes (p-value < 0.05, |log2FC| > 0.585) was

identified by using the limma package of R based on RNA-seq data of bladder cancer samples obtained from TCGA. After considering the list of immune-related genes obtained from ImmPort in context, immune-related differentially expressed genes were obtained and analyzed by using Gene Ontology (GO) and Kyoto Encyclopedia of Genes and Genomes (KEGG) analysis.

The core genes were then analyzed by WGCNA. First, a similarity matrix was constructed using the expression data by calculating the Pearson correlation coefficient between the two genes. Then, the similarity matrix was converted into an adjacency matrix with a network type of sign and a soft threshold of $\beta = 5$, and then into a Topological Overlap Metric (TOM) describing the degree of association between genes. The genes are clustered with 1-TOM as the distance, and then dynamic pruning trees are constructed for module identification. Finally, five modules were identified by setting the merging threshold function to 0.25. Based on the genes of significantly related modules (yellow module and blue-green module), the network was constructed using the edge between two genes with weight > 0.2. The top 50 genes in the network in terms of ranking are the central genes. The best cut-off value of Overall Survival (OS) was calculated for each core gene using R language, and immune-related core genes significantly associated with survival were screened for further analysis ($p < 0.05$, log-rank test). To reveal the associated genetic alterations, somatic mutations in 29 immune-associated HUB genes were analyzed using R.

2.3. Construction and Validation of Immune-Related Gene Prognostic Index (IRGPI)

Among the immune-related core genes that had been screened above, genes with significant effects on OS were screened and IRGPI was constructed by multifactorial Cox regression analysis. The IRGPI of each sample was obtained by multiplying the expression values of specific genes by their weights in the Cox model and then summing them. The prognostic power of the IRGPI was assessed by performing log-rank tests on the K-M survival curves of the TCGA and GEO cohorts. To verify the independent prognostic value of IRGPI, one- and multifactor Cox regression analyses were performed. Independent immune-related genes associated with prognosis were identified by univariate and multifactorial Cox regression. Then, risk score models were constructed based on the expression levels and coefficients of these genes. The risk score was calculated for each BLCA patient using the following formula: risk score = $\beta 1$ * Exp1 + $\beta 2$ * Exp2 + βi * Expi, where β denotes the independent prognosis-related RBP, the coefficient value proficiency represents the expression level of the prognosis-independent gene, and i represents the ith gene.

2.4. Comprehensive Analysis of Molecular Immune Characteristics of Different IRGPI Subgroups and ICI Treatment

In the signaling pathway analysis, the samples from the high and low IRGPI

scoring groups were first analyzed for differential expression using R's Limma package to identify signaling pathways involving differentially expressed genes, and then Gene Set Enrichment Analysis (GSEA) was performed on the KEGG and HARMARK gene sets using R's clusterProfiler package ($p < 0.05$ and fdr < 0.25). Single-sample GSEA (SsGSEA) analysis was performed with R's GSVA package for several representative gene sets, and survival differences were analyzed with Kaplan-Meier survival curves. Mutation data from two IRGPI subgroups were analyzed using R's Maftools package, and IRGPI scores were correlated with PD-L1 expression and Total Mutation Load (TMB).

To characterize the immune properties of 414 bladder cancer samples, their expression data were imported into CiberSort (https://cibersortx.stanford.edu/) and iterated 1000 times to estimate the relative proportions of 22 immune cell types. We then compared the relative proportions of the 22 immune cells and clinicopathological factors between the two IRGPI subgroups.

To further determine the immune and molecular functions between IRGPI subgroups, we performed ssGSEA on certain gene signatures and compared the scores between the two IRGPI subgroups.

To explore the value of IRGPI in the prognosis of patients after immunotherapy, we also performed time-related ROC curve analysis, obtained the Area under the Curve (AUC), and compared the prognostic value between IRGPI, TIDE and TIS with the time ROC package of R. The TIDE score was calculated online (http://tide.dfci.harvard.edu/login/), and the TIS score was calculated as the mean of log2-scale normalized expression of 18 marker genes.

2.5. Statistical Analysis

Independent t-test was used for comparison of continuous variables between two groups. Categorical data were tested by chi-square test. The Wilcoxon test was used for comparison of TIDE scores between groups. Univariate survival analysis was performed using Kaplan-Meier survival analysis and log-rank test. Multifactorial survival analysis was performed using Cox regression model. Two-sided p values < 0.05 were considered significant.

3. Results

3.1. Immune-Associated Central Genes

In differential expression analysis (414 tumors vs. 19 normal controls), a total of 407 differentially expressed immune-related genes were obtained by crossing these genes with the list of immune-related genes obtained from ImmPort. To obtain immune-related central genes, WGCNA analysis was performed on candidate genes (n = 407). The log log(k) of nodes with connectivity k was negatively correlated with the log log(P(k)) of node probabilities and the correlation coefficient was greater than 0.85. Candidate genes were assigned to 5 modules. The yellow and blue-green modules that were closely associated with bladder tumors were selected for further analysis based on the Pierson correlation coeffi-

cient between module and sample characteristics for each module, and genes in these modules were selected for further analysis.

Differentially expressed RBPs were submitted to the STRING database (https://cn.string-db.org/) for PPI detection. PPI networks were then constructed and visualized using Cytoscape 3.7.0. The Molecular Complexity Detection (MCODE) plugin was used to screen key modules from the PPI network with both MCODE scores and node counts > 5. $p < 0.05$ was considered statistically significant. We obtained the top 50 immune-related hub genes with a threshold of degree > 20. As determined by K-M analysis, expression of 29 immune-related HUB genes was strongly associated with OS in bladder cancer patients ($p < 0.05$, logarithmic test, **Figure 1(a)**).

Then, we explored the characteristics of the 29 immune-associated HUB genes. As shown in **Figure 1(b)**, most of the 29 immune-related core genes had missense mutations, among which AHNAK, PDGFRA, SLIT2 and NRP2 had high mutation rates, especially AHNAK mutation rate reached 9%.

Multifactorial Cox regression analysis was performed on 29 immune-related core genes; six independent genes associated with prognosis were identified by multifactorial Cox regression. We developed a prognosis-related risk score model based on the six independent prognosis-related genes. In the model, IRGPI = expression level of AHNAK * 0.49 + expression level of ILK * (−0.24) + expression level of OGN * (−0.18) + expression level of PDGFD * 0.29 + expression level of PPARGC1B * (−0.46) + expression level of JAM3 * 0.30.

Univariate COX regression analysis in the TCGA cohort showed that age, clinical stage and IRGPI risk coefficient were significantly associated with the prognosis of bladder tumors (**Figure 1(c)**). Further multivariate Cox regression analysis also showed that IRGPI and clinical stage were independent predictors of bladder cancer prognosis (**Figure 1(d)**). These results suggest that IRGPI and clinical stage are likely to be associated and could be used as bladder tumor a valid biomarker of prognosis. Patient PI values were calculated and patients were divided into high and low risk groups using the median as the cut-off value. Clinical staging of bladder cancer was divided into stage 1 - 4, relative to the two IRGPI subgroups, with stage II predominantly in the low IRGPI subgroup, and stage III, stage IV predominantly in the high IRGPI subgroup ($p < 0.001$, chi-square test, **Figure 1(e)**).

PD-L1 expression was higher in the subgroup with high IRGPI than in the subgroup with low IRGPI, with statistical value ($p = 0.011$), and IRGPI score was correlated with PD-L1 ($R = 0.17$, $p = 0.00073$, **Figure 2(a)**). TMB was slightly higher in the subgroup with low IRGPI, without statistical value ($p = 0.074$), and with IRGPI score was slightly correlated ($R = 0.13$, $p = 0.0089$, **Figure 2(b)**).

Kaplan-Meier survival analysis was performed. One-way cox regression analysis revealed that the high-risk group had lower OS than the low-risk group ($p < 0.001$, log test, **Figure 3(a)**), and then, using the GEO cohort as a validation cohort, the results were consistent with the TCGA cohort ($p < 0.001$, log test, **Figure 3(b)**).

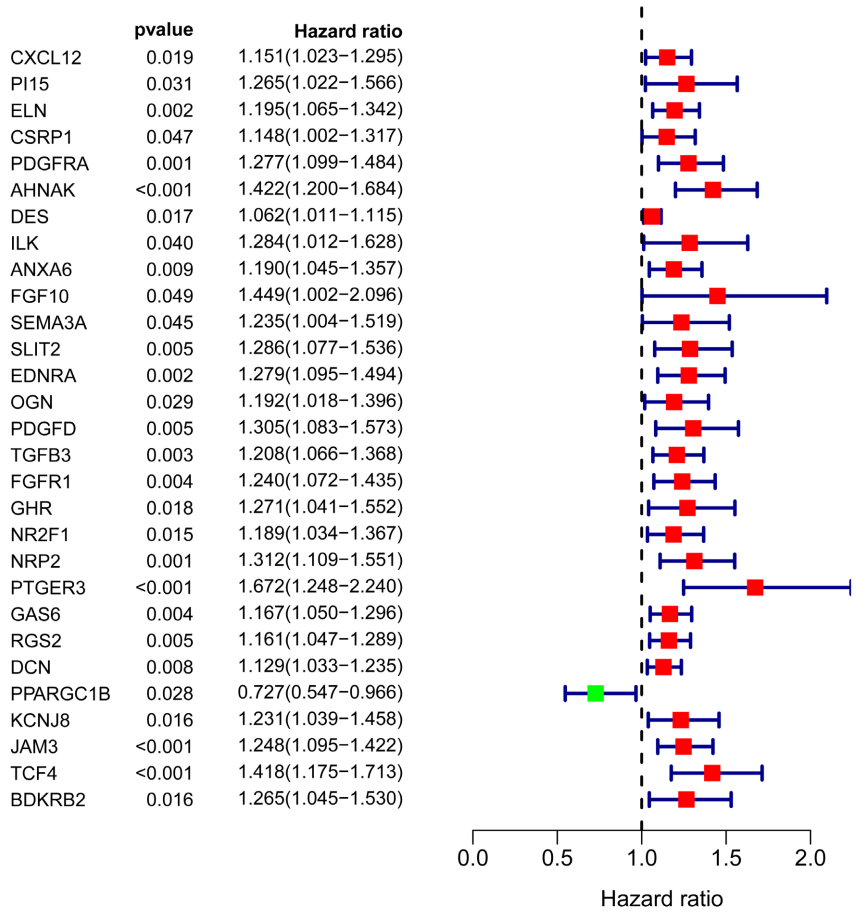
pvalue
Hazard ratio
CXCL12 0.019 1.151(1.023−1.295)
PI15 0.031 1.265(1.022−1.566)
ELN 0.002 1.195(1.065−1.342)
CSRP1 0.047 1.148(1.002−1.317)
PDGFRA 0.001 1.277(1.099−1.484)
AHNAK <0.001 1.422(1.200−1.684)
DES 0.017 1.062(1.011−1.115)
ILK 0.040 1.284(1.012−1.628)
ANXA6 0.009 1.190(1.045−1.357)
FGF10 0.049 1.449(1.002−2.096)
SEMA3A 0.045 1.235(1.004−1.519)
SLIT2 0.005 1.286(1.077−1.536)
EDNRA 0.002 1.279(1.095−1.494)
OGN 0.029 1.192(1.018−1.396)
PDGFD 0.005 1.305(1.083−1.573)
TGFB3 0.003 1.208(1.066−1.368)
FGFR1 0.004 1.240(1.072−1.435)
GHR 0.018 1.271(1.041−1.552)
NR2F1 0.015 1.189(1.034−1.367)
NRP2 0.001 1.312(1.109−1.551)
PTGER3 <0.001 1.672(1.248−2.240)
GAS6 0.004 1.167(1.050−1.296)
RGS2 0.005 1.161(1.047−1.289)
DCN 0.008 1.129(1.033−1.235)
PPARGC1B 0.028 0.727(0.547−0.966)
KCNJ8 0.016 1.231(1.039−1.458)
JAM3 <0.001 1.248(1.095−1.422)
TCF4 <0.001 1.418(1.175−1.713)
BDKRB2 0.016 1.265(1.045−1.530)
0.0
0.5
1.0
1.5
2.0
Hazard ratio

(a)

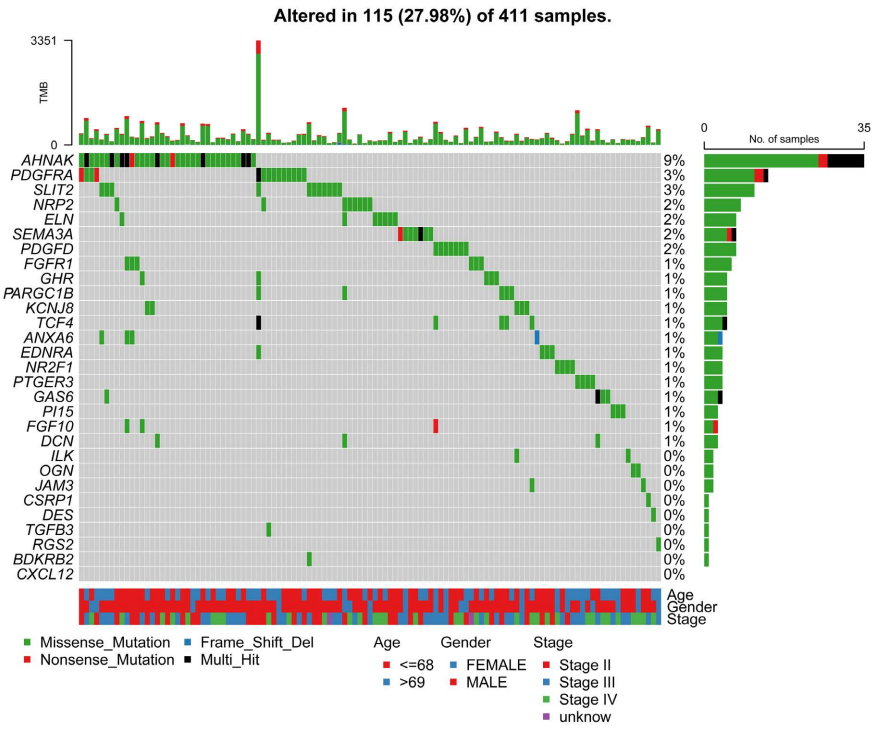
Altered in 115 (27.98%) of 411 samples.
TMB
3351
0
No. of samples
0
35
AHNAK 9%
PDGFRA 3%
SLIT2 3%
NRP2 2%
ELN 2%
SEMA3A 2%
PDGFD 2%
FGFR1 1%
GHR 1%
PARGC1B 1%
KCNJ8 1%
TCF4 1%
ANXA6 1%
EDNRA 1%
NR2F1 1%
PTGER3 1%
GAS6 1%
PI15 1%
FGF10 1%
DCN 1%
ILK 0%
OGN 0%
JAM3 0%
CSRP1 0%
DES 0%
TGFB3 0%
RGS2 0%
BDKRB2 0%
CXCL12 0%
Age
Gender
Stage
Missense_Mutation
Nonsense_Mutation
Frame_Shift_Del
Multi_Hit
Age
<=68
>69
Gender
FEMALE
MALE
Stage
Stage II
Stage III
Stage IV
unknow

(b)

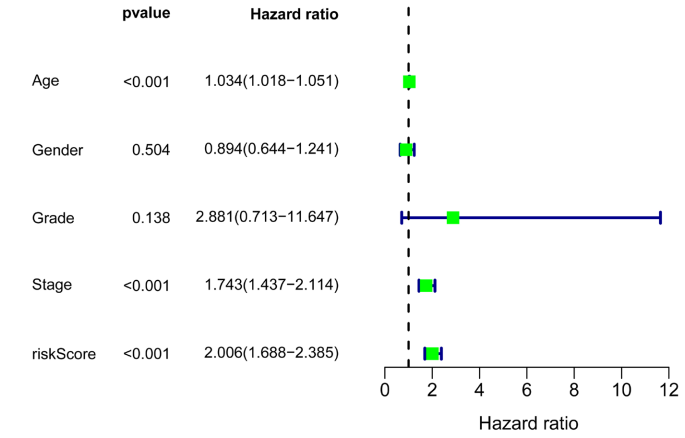

(c)

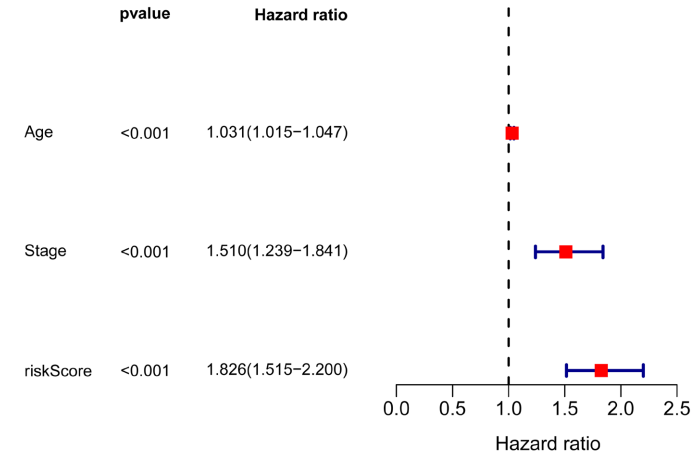

(d)

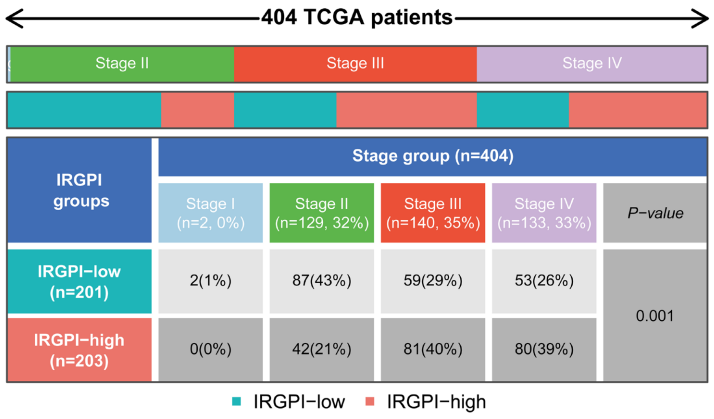

(e)

Figure 1. (a) Univariate COX analysis of 29 immune-related hub genes. (b) Relationship between 29 genes with immune-associated mutations and clinicopathological factors in bladder cancer samples, with the mutation rate shown on the right and the total number of mutations shown above, and color coding indicates the mutation type. (c) Univariate Cox analysis of clinicopathological factors and riskScore. (d) Multivariate Cox analysis for factors significant in univariate Cox analysis ($p < 0.05$). (e) Association with clinical staging in different IRGPI subgroups.

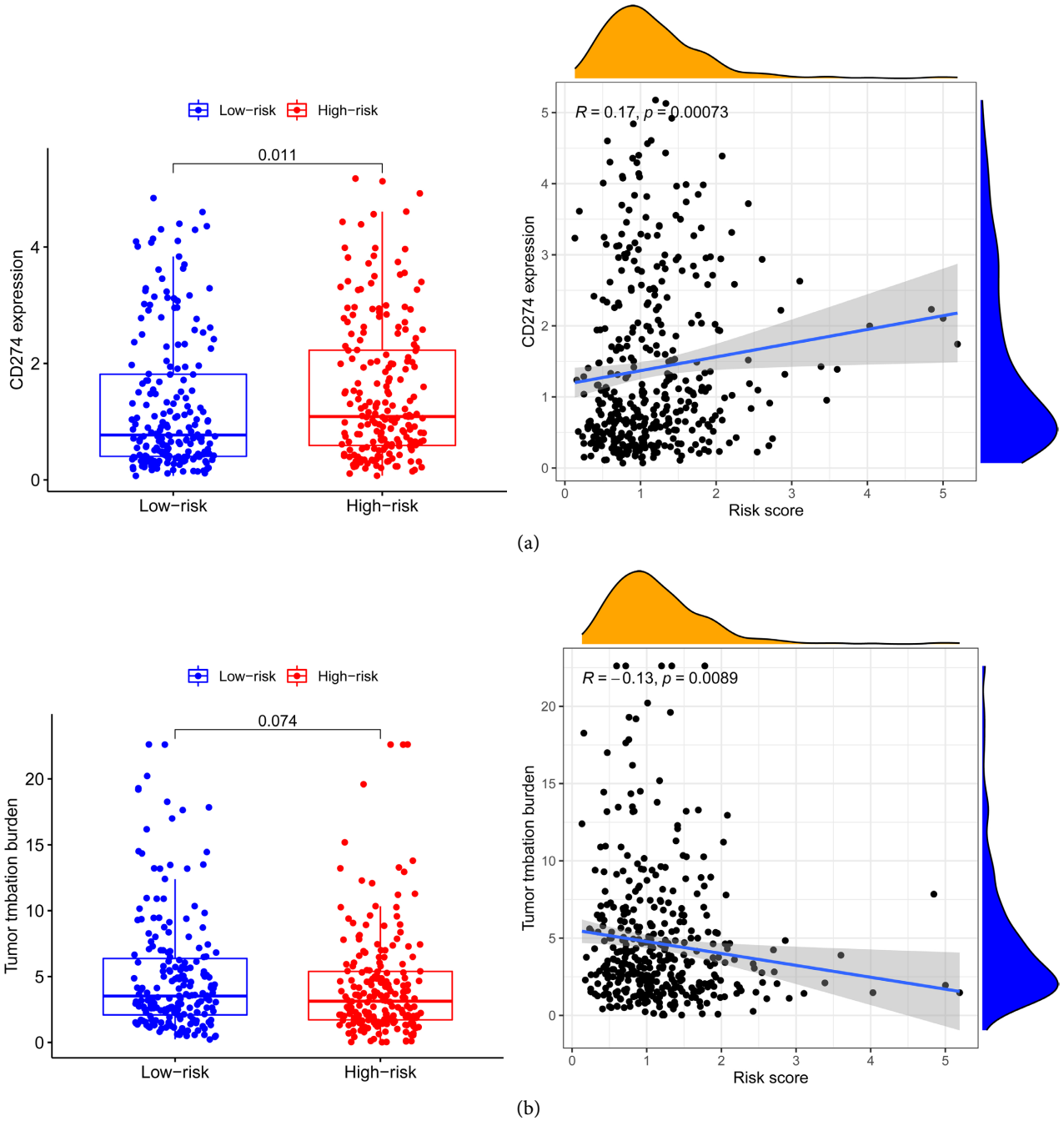

Figure 2. Relationship between IRGPI and total mutation burden and PDL1 expression. (a) Correlation analysis between IRGPI and total mutation burden; (b) Correlation analysis between IRGPI and PD-L1 expression.

3.2. Immunological Characteristics of the IRGPI Subgroup

The CIBERSORT algorithm was applied to calculate the proportion of 22 immune cells, and the Wilconxon test was used to compare the distribution of immune cells in different IRGPI subgroups. Resting memory CD4T cells, M0 macrophages, and M2 macrophages were more abundant in the subgroup with high IRGPI, while CD8T cells, and activated memory CD4T cells were more abundant in the subgroup with low IRGPI (**Figures 4(a)-(c)**).

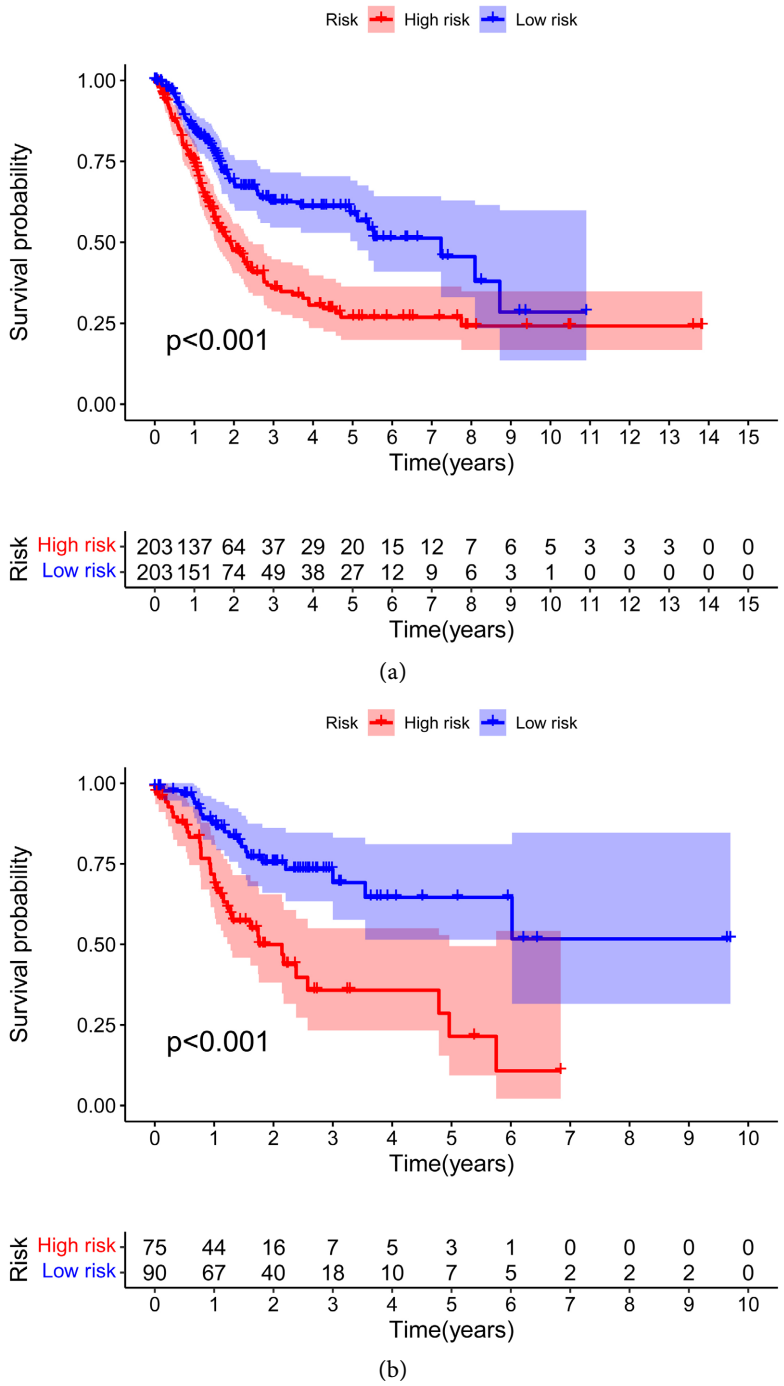

Figure 3. (a) K-M survival analysis of the IRGPI subgroup in the TCGA cohort. (b) K-M survival analysis of the IRGPI subgroup in the GEO cohort.

In the K-M survival analysis of 22 immune cells in both IRGPI subgroups, it was found that high infiltration of memory B cells, M0 macrophages, M2 macrophages, resting mast cells, monocytes, and neutrophils in the low IRGPI group had better OS compared with high infiltration of plasma cells, activated memory CD4 T cells, CD8 T cells, and follicular helper T cells in the high IRGPI group ($p < 0.05$, log test, **Figure 4(d)**).

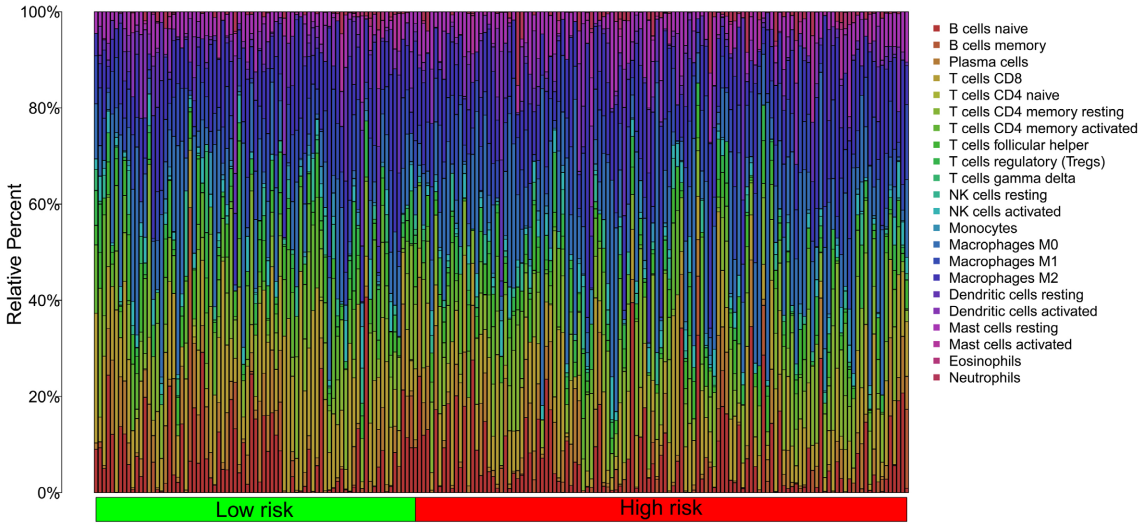
100%
80%
60%
40%
20%
0%
Relative Percent
Low risk
High risk
B cells naive
B cells memory
Plasma cells
T cells CD8
T cells CD4 naive
T cells CD4 memory resting
T cells CD4 memory activated
T cells follicular helper
T cells regulatory (Tregs)
T cells gamma delta
NK cells resting
NK cells activated
Monocytes
Macrophages M0
Macrophages M1
Macrophages M2
Dendritic cells resting
Dendritic cells activated
Mast cells resting
Mast cells activated
Eosinophils
Neutrophils

(a)

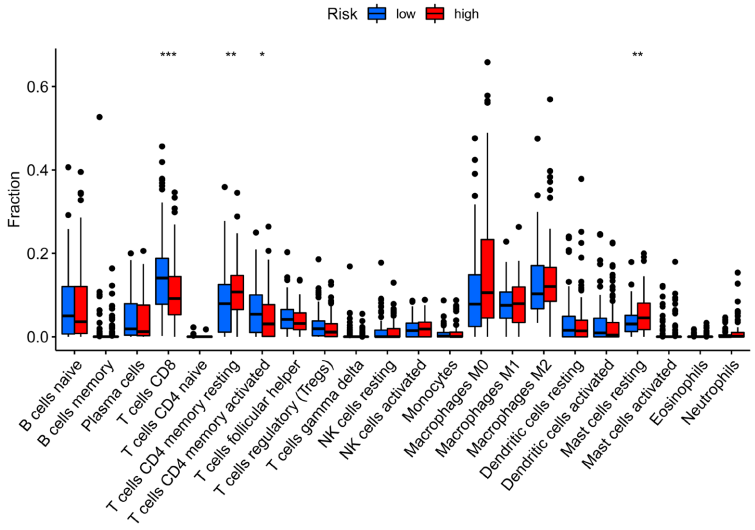
Risk low high
Fraction
0.0
0.2
0.4
0.6
B cells naive
B cells memory
Plasma cells
T cells CD8
T cells CD4 naive
T cells CD4 memory resting
T cells CD4 memory activated
T cells follicular helper
T cells regulatory (Tregs)
T cells gamma delta
NK cells resting
NK cells activated
Monocytes
Macrophages M0
Macrophages M1
Macrophages M2
Dendritic cells resting
Dendritic cells activated
Mast cells resting
Mast cells activated
Eosinophils
Neutrophils

(b)

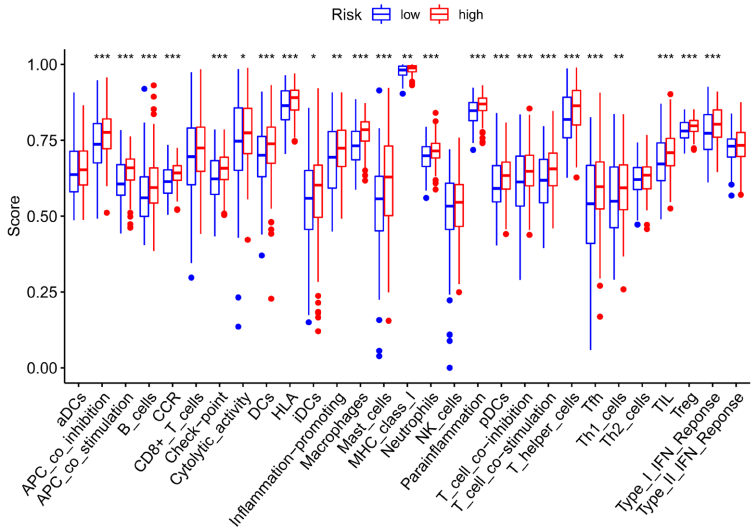
Risk low high
Score
0.00
0.25
0.50
0.75
1.00
aDCs
APC_co_inhibition
APC_co_stimulation
B_cells
CCR
CD8+_T_cells
Check-point
Cytolytic_activity
DCs
HLA
iDCs
Inflammation-promoting
Macrophages
Mast_cells
MHC_class_I
Neutrophils
NK_cells
Parainflammation
pDCs
T_cell_co-inhibition
T_cell_co-stimulation
T_helper_cells
Tfh
Th1_cells
Th2_cells
TIL
Treg
Type_I_IFN_Reponse
Type_II_IFN_Reponse

(c)

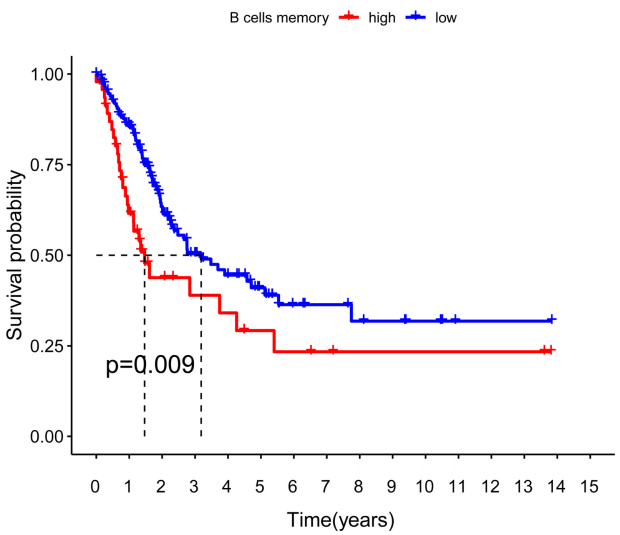
B cells memory high low
Survival probability
1.00
0.75
0.50
0.25
0.00
p=0.009
0 1 2 3 4 5 6 7 8 9 10 11 12 13 14 15
Time(years)

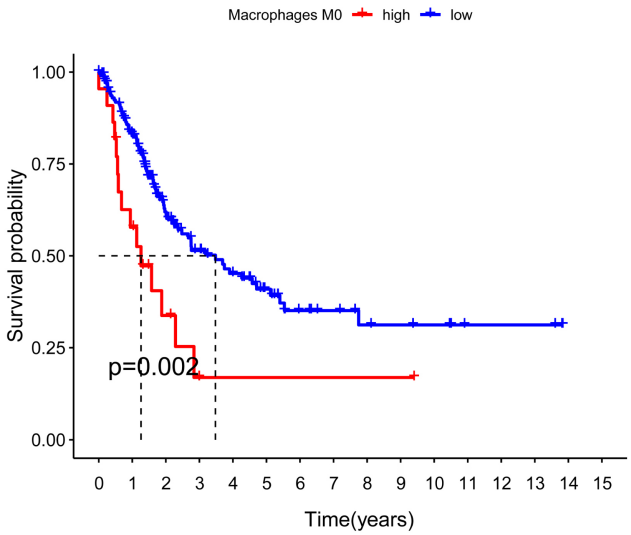
Macrophages M0 high low
Survival probability
1.00
0.75
0.50
0.25
0.00
p=0.002
0 1 2 3 4 5 6 7 8 9 10 11 12 13 14 15
Time(years)

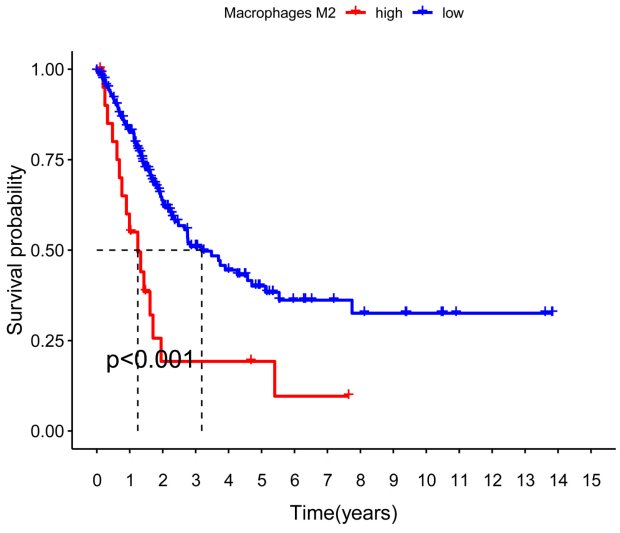
Macrophages M2 high low
Survival probability
1.00
0.75
0.50
0.25
0.00
p<0.001
0 1 2 3 4 5 6 7 8 9 10 11 12 13 14 15
Time(years)

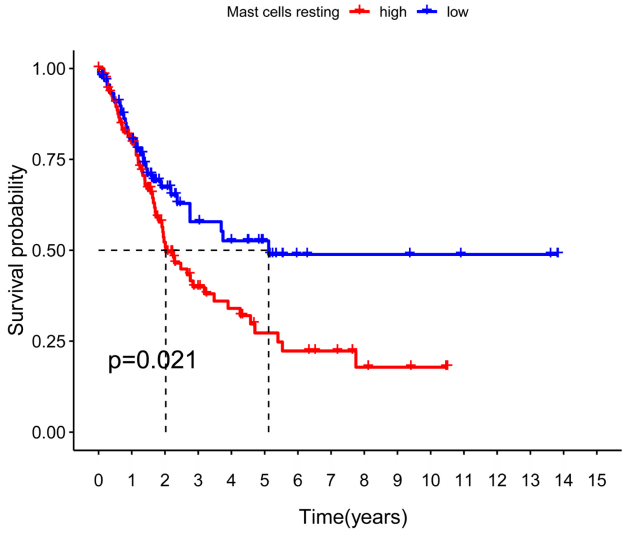
Mast cells resting high low
Survival probability
1.00
0.75
0.50
0.25
0.00
p=0.021
0 1 2 3 4 5 6 7 8 9 10 11 12 13 14 15
Time(years)

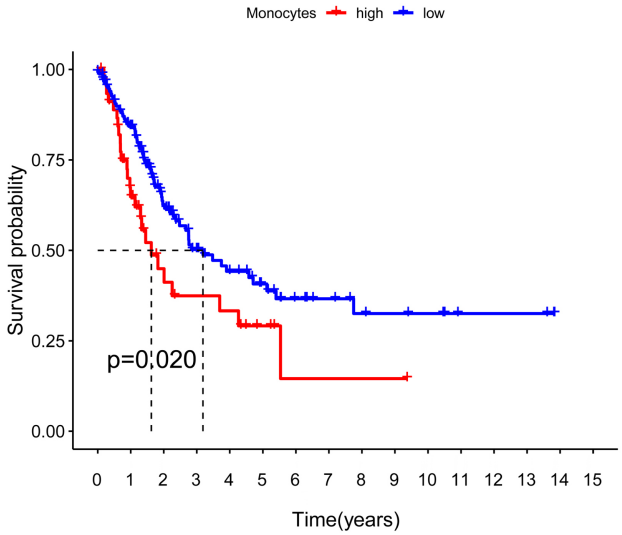
Monocytes high low
Survival probability
1.00
0.75
0.50
0.25
0.00
p=0.020
0 1 2 3 4 5 6 7 8 9 10 11 12 13 14 15
Time(years)

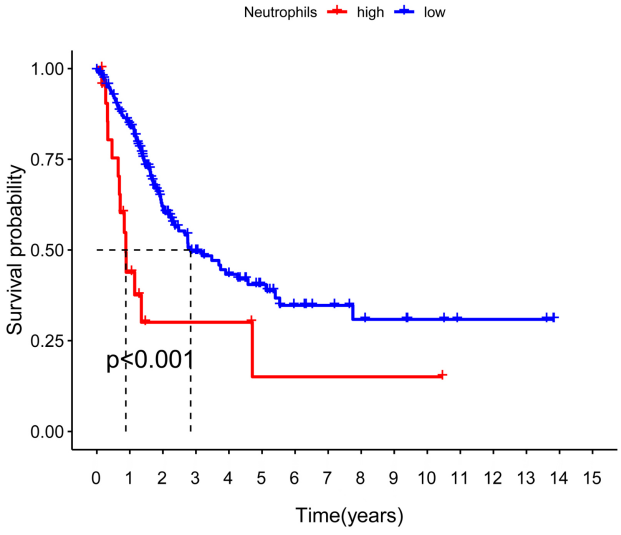
Neutrophils high low
Survival probability
1.00
0.75
0.50
0.25
0.00
p<0.001
0 1 2 3 4 5 6 7 8 9 10 11 12 13 14 15
Time(years)

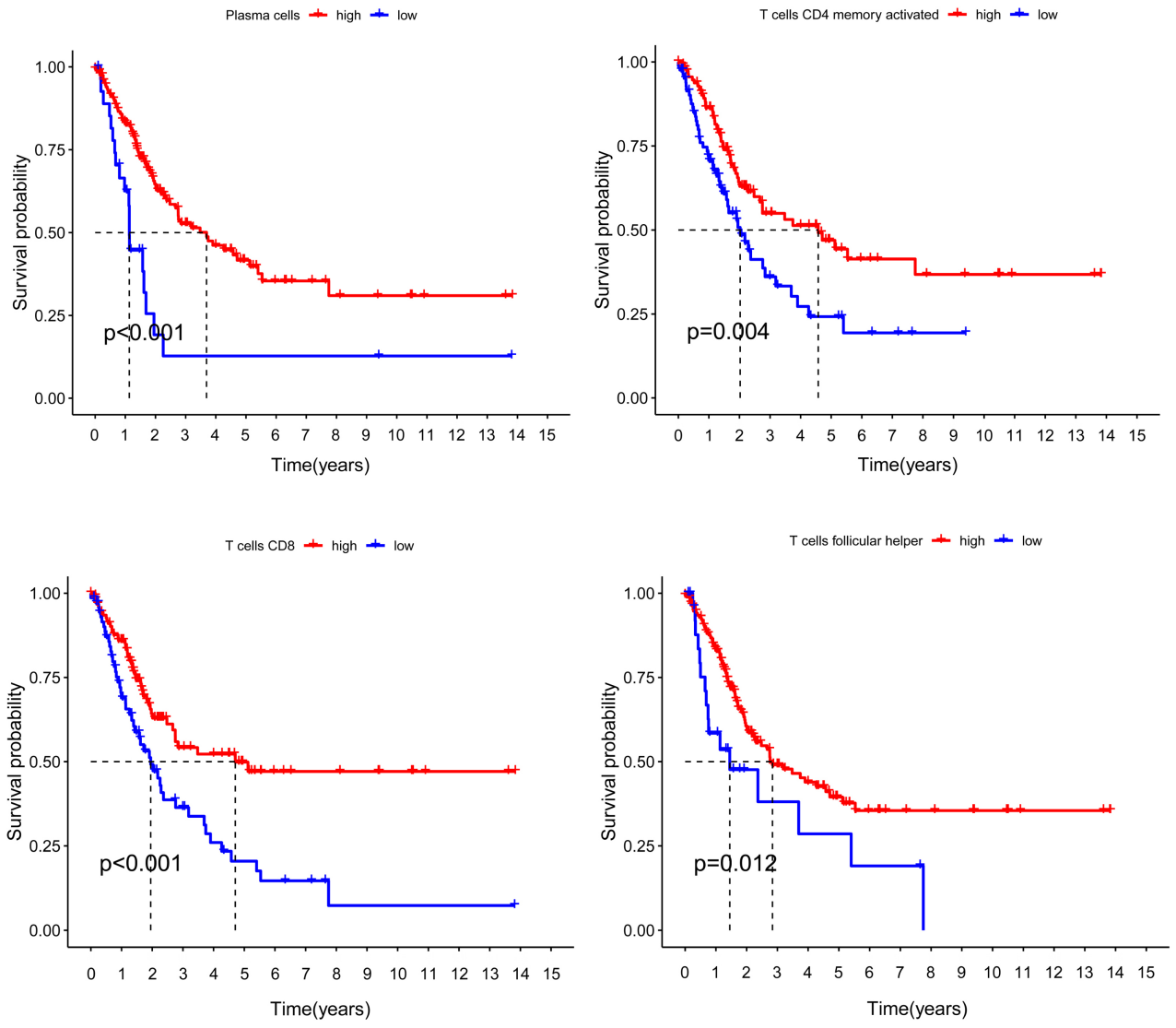

(d)

Figure 4. (a) IRGPI subgroups and proportion of 22 immune cells in bladder cancer patients in the TCGA cohort. (b) Proportions of 22 immune cell species in different IRGPI subgroups, with thick lines representing median values. The bottom and top of the box are the 25th and 75th percentile (interquartile range), respectively. Differences between the two subgroups were assessed by Wilcoxon test (ns, not significant; *, $p < 0.05$; **, $p < 0.01$; ***, $p < 0.001$; ****, $p < 0.0001$). (c) Molecular and immune-related functions of different IRGPI subgroups. Gene sets for molecular and immune-related functions were analyzed by single simple gene set enrichment analysis (ssGSEA) and then compared between different IRGPI subgroups. The scattered points represent the ssGSEA scores of the two subgroups. The thick line represents the median. The bottom and top of the box are the 25th and 75th percentile (interquartile range), respectively. Statistically significant differences between the two subgroups were assessed with the Wilcoxon test (ns: not significant, *$p < 0.05$, ** $p < 0.01$, *** $p < 0.001$). (d) Kaplan-Meier survival curves of specific immune cells in different IRGPI subgroups.

3.3. ICI Treatment Efficiency in the IRGPI Subgroup

The subgroup with low IRGPI had lower TIDE scores than the subgroup with high IRGPI, meaning that patients with low IRGPI were more suitable for ICI therapy (**Figure 5**). The subgroup with high IRGPI had higher T-cell rejection scores and T-cell dysfunction. There was no difference in microsatellite instability

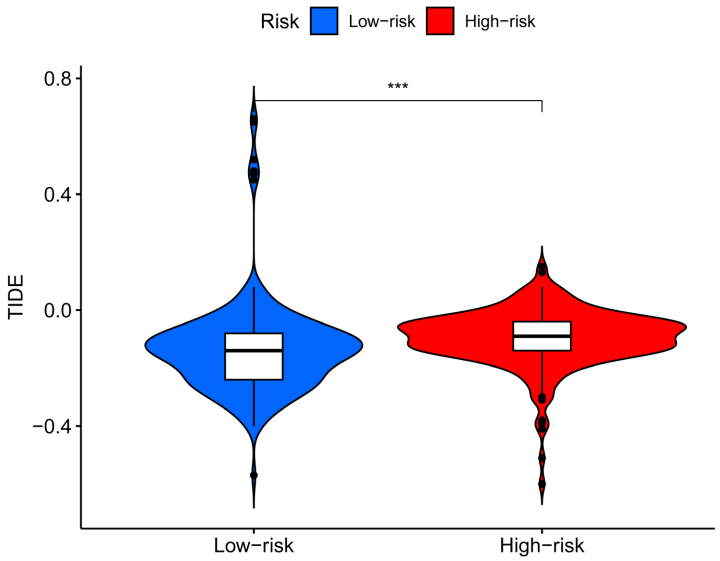
Risk
Low−risk
High−risk
0.8
0.4
0.0
−0.4
TIDE
***
Low−risk
High−risk

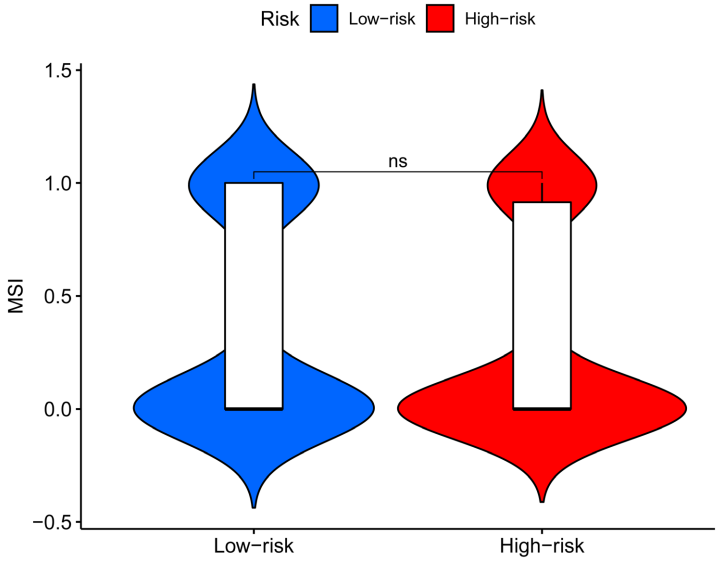
Risk
Low−risk
High−risk
1.5
1.0
0.5
0.0
−0.5
MSI
ns
Low−risk
High−risk

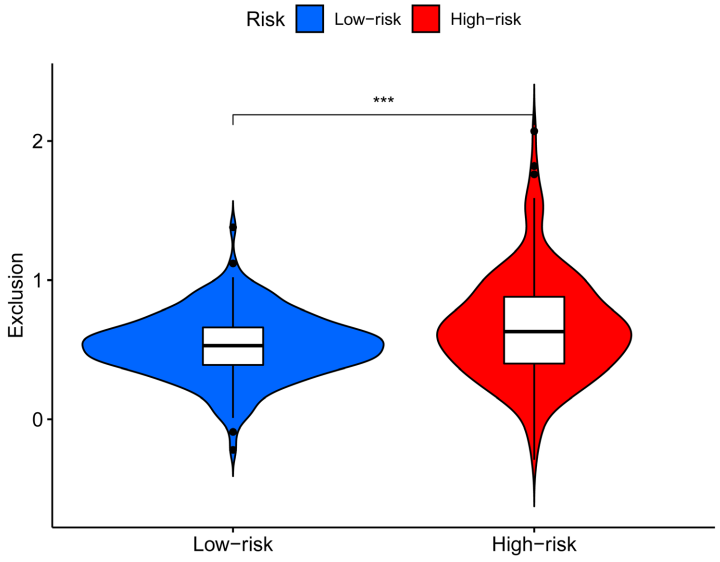
Risk
Low−risk
High−risk
2
1
0
Exclusion
***
Low−risk
High−risk

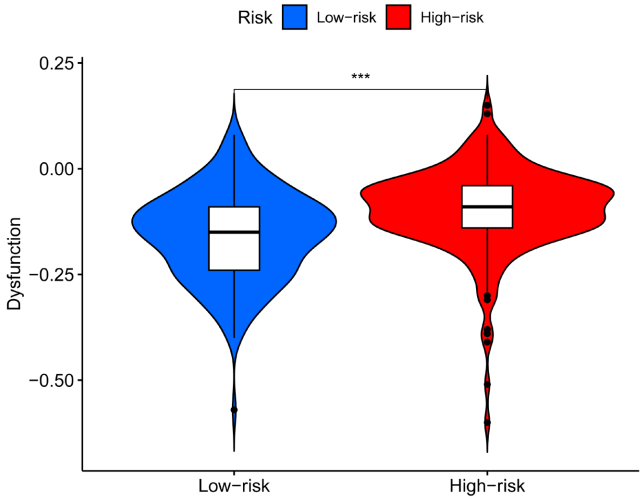

(a)

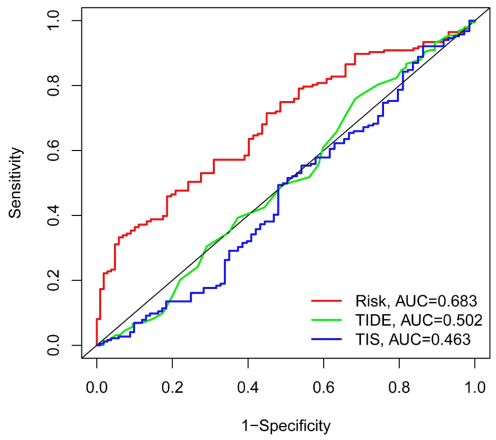

(b)

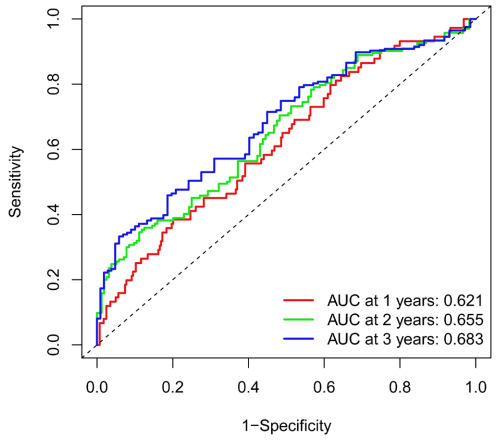

(c)

Figure 5. Prognostic value of patients treated with IRGPI against PD-L1. (a) TIDE, MSI and T-cell rejection and dysfunction scores in different IRGPI subgroups. Scores were compared between the two IRGPI subgroups by Wilcoxon test (ns, no significance; *, $p < 0.05$; ***, $p < 0.001$). (b) Comparison of ROC analysis of IRGPI, TIS and TIDE for TCGA bladder cancer cohort. (c) ROC analysis of OS at 1-, 2-, and 3-year follow-up for the TCGA bladder cancer cohort by IRGPI.

(MSI) scores between the two subgroups. In the analysis of the TCGA bladder cancer patient cohort, IRGPI had a significantly higher predictive value than TIDE and TIS, with the best at 3 years of follow-up.

4. Conclusions

In this paper, we found six immune-related prognostic genes to establish IRGPI with accuracy and validity in predicting the prognosis of bladder cancer and the efficacy of ICI treatment. Among the six core genes, the mutation rate of AHNAK reached 9%. As a tumor suppressor, AHNAK, also known as desmoglein, negatively regulates triple-negative breast cancer cell proliferation, triple-negative breast cancer xenograft growth, and metastasis through different signaling pathways [13]. In malignant tumors, AHNAK lacks uniform expression and has different intracellular localizations depending on the tumor cell type [14] [15] [16]. AHNAK in neuroblastoma cell lines is described as a nuclear protein whose expression is significantly suppressed [17], whereas, in a study on melanoma, an immune response was observed mainly in the cytoplasm of normal cells, in contrast to the disappearance of expression in melanoma cells [18].

IRGPI is associated with the infiltration of multiple immune cells [19], which contributes to further revealing the role and interrelationship of immune cells in the immune microenvironment of bladder cancer, and as the risk value of IRGPI increases, the later the clinical stage of the patient, the progressive impairment of the main immune function of the body leading to tumor development and metastasis, etc., these differences in the level of infiltration of immune-related cells may indicate the risk value potential immune mechanisms, which could have significant clinical application by detecting relevant infiltrating immune cells in bladder cancer patients to distinguish high and low-risk groups or as immune targets.

The tumor microenvironment consists of the tumor and its surrounding fibroblasts, adipocytes, immune cells, extracellular matrix, and tumor vasculature, which are the environment in which tumors grow, metastasize and evolve [20]. Among them, immune cells, inflammatory cells, and cytokines, which are closely related to immune response, constitute the tumor immune microenvironment and are mainly involved in tumor immune editing [21] [22]. The tumor microenvironment plays an important role in the regulation of PD-L1, and its composition is closely related to the efficacy of ICIs [23].

Tumor-associated macrophages (TAMs), which can be differentiated from CD14-positive monocytes or MDSC, similarly exert immunosuppressive effects and promote tumor metastasis. TAMs are classified into pro-inflammatory type M1 and pro-tumor type M2 according to their polarization status. In contrast, the M2-type TAM, which is subject to chemokine (CCL2), IL-10, and TGF-β-induced polarization, can suppress T-cell immune responses and promote angiogenesis by secreting IL-4, IL-5, IL-6, and ARG1 [24]. M1-macrophages suppress T-cell immune responses and promote angiogenesis by promoting IL-1β, TNF-α IL-6,

IL-12, and other cytokine expressions as well as enhancing the function of helper T cell 1 (Th1) to exert anti-tumor effects, and M2-macrophages exert immunosuppressive functions by promoting the expression of immunosuppressive cytokines such as TGF-β1 and IL-10, thereby promoting tumor progression and metastasis [25]. TAMs were found to be abundant in bladder cancer in this study, and M2 macrophages were predominant, which is consistent with previous studies.

In recent years, there has been a lot of exploration of immunotherapeutic markers, and new markers have emerged, such as TIDE and TIS. The Tumor Immune Dysfunction and Exclusion (TIDE) predicted outcomes in melanoma patients treated with first-line anti-PD1 or anti-CTLA4 more accurately than other biomarkers such as PD-L1 levels and mutational load [26]. The results of the RATIONALE-307 phase III clinical trial results confirmed a strong association between TIS score and PD-1 inhibitor combination chemotherapy in delivering significant survival benefits to patients with sq-NSCLC [27]. In the present study, the predictive value of IRGPI was comparable to TIDE and TIS, and at longer follow-up, it proved to be a better predictor of OS, however, as an exploratory study the value of IRGPI in bladder cancer needs to be validated in a multicenter clinical study with a large sample.

In summary, IRGPI established by six immune-related prognostic genes can accurately predict the prognosis of clinical bladder cancer to a certain extent, which will provide new research ideas and directions for the etiology, pathogenesis, individualized immunotherapy, and prognostic judgment of bladder cancer.

Ethics Approval and Consent to Participate

The data used in our study were obtained from public databases TCGA and GEO, therefore, ethical approval was not required.

Conflicts of Interest

The authors declare no conflicts of interest regarding the publication of this paper.

References

[1] Bray, F., Ferlay, J., Soerjomataram, I., Siegel, R.L., Torre, L.A. and Jemal, A. (2018) Global Cancer Statistics 2018: GLOBOCAN Estimates of Incidence and Mortality Worldwide for 36 Cancers in 185 Countries. *CA*: *A Cancer Journal for Clinicians*, **68**, 394-424. https://doi.org/10.3322/caac.21492

[2] Witjes, J.A., Bruins, H.M., Cathomas, R., Compérat, E.M., Cowan, N.C., Gakis, G., *et al.* (2021) European Association of Urology Guidelines on Muscle-invasive and Metastatic Bladder Cancer: Summary of the 2020 Guidelines. *European Urology*, **79**, 82-104. https://doi.org/10.1016/j.eururo.2020.03.055

[3] Lerner, S.P. and Robertson, A.G. (2016) Molecular Subtypes of Non-muscle Invasive Bladder Cancer. *Cancer Cell*, **30**, 1-3. https://doi.org/10.1016/j.ccell.2016.06.012

[4] Robertson, A.G., Kim, J., Al-Ahmadie, H., Bellmunt, J., Guo, G., Cherniack, A.D., *et*

al. (2018) Comprehensive Molecular Characterization of Muscle-Invasive Bladder Cancer. *Cell*, **174**, 1033. https://doi.org/10.1016/j.cell.2018.07.036

[5] Song, D., Powles, T., Shi, L., Zhang, L., Ingersoll, M.A. and Lu, Y.J. (2019) Bladder Cancer, a Unique Model to Understand Cancer Immunity and Develop Immunotherapy Approaches. *The Journal of Pathology*, **249**, 151-165. https://doi.org/10.1002/path.5306

[6] Bellmunt, J., de Wit, R., Vaughn, D.J., Fradet, Y., Lee, J.L., Fong, L., *et al*. (2017) Pembrolizumab as Second-Line Therapy for Advanced Urothelial Carcinoma. *The New England Journal of Medicine*, **376**, 1015-1026. https://doi.org/10.1056/NEJMoa1613683

[7] Paré, L., Pascual, T., Seguí, E., Teixidó, C., Gonzalez-Cao, M., Galván, P., *et al*. (2018) Association between *PD1* mRNA and Response to Anti-PD1 Monotherapy across Multiple Cancer Types. *Annals of Oncology*, **29**, 2121-2128. https://doi.org/10.1093/annonc/mdy335

[8] Sun, R., Limkin, E.J., Vakalopoulou, M., Dercle, L., Champiat, S., Han, S.R., *et al*. (2018) A Radiomics Approach to Assess Tumour-Infiltrating CD8 Cells and Response to Anti-PD-1 or Anti-PD-L1 Immunotherapy: An Imaging Biomarker, Retrospective Multicohort Study. *The Lancet Oncology*, **19**, 1180-1191. https://doi.org/10.1016/S1470-2045(18)30413-3

[9] Tian, Z., Meng, L., Long, X., Diao, T., Hu, M., Wang, M., *et al*. (2020) Identification and Validation of an Immune-Related Gene-Based Prognostic Index for Bladder Cancer. *The American Journal of Translational Research*, **12**, 5188-5204. https://doi.org/10.2139/ssrn.3550003

[10] Nishino, M., Ramaiya, N.H., Hatabu, H. and Hodi, F.S. (2017) Monitoring Immune-Checkpoint Blockade: Response Evaluation and Biomarker Development. *Nature Reviews Clinical Oncology*, **14**, 655-668. https://doi.org/10.1038/nrclinonc.2017.88

[11] Kalbasi, A. and Ribas, A. (2020) Tumour-Intrinsic Resistance to Immune Checkpoint Blockade. *Nature Reviews Immunology*, **20**, 25-39. https://doi.org/10.1038/s41577-019-0218-4

[12] Tran, L., Xiao, J.F., Agarwal, N., Duex, J.E. and Theodorescu, D. (2021) Advances in Bladder Cancer Biology and Therapy. *Nature Reviews Cancer*, **21**, 104-121. https://doi.org/10.1038/s41568-020-00313-1

[13] Chen, B., Wang, J., Dai, D., Zhou, Q., Guo, X., Tian, Z., *et al*. (2017) AHNAK Suppresses Tumour Proliferation and Invasion by Targeting Multiple Pathways in Triple-Negative Breast Cancer. *Journal of Experimental & Clinical Cancer Research*, **36**, Article No. 65. https://doi.org/10.1186/s13046-017-0522-4

[14] Huang, Y., Laval, S.H., van Remoortere, A., Baudier, J., Benaud, C., Anderson, L.V.B., *et al*. (2007) AHNAK, a Novel Component of the Dysferlin Protein Complex, Redistributes to the Cytoplasm with Dysferlin During Skeletal Muscle Regeneration. *The FASEB Journal*, **21**, 732-742. https://doi.org/10.1096/fj.06-6628com

[15] Nie, Z., Ning, W., Amagai, M. and Hashimoto, T. (2000) C-Terminus of Desmoyokin/AHNAK Protein Is Responsible for Its Translocation between the Nucleus and Cytoplasm. *Journal of Investigative Dermatology*, **114**, 1044-1049. https://doi.org/10.1046/j.1523-1747.2000.00949.x

[16] Davis, T.A., Loos, B. and Engelbrecht, A.M. (2014) AHNAK: The Giant Jack of All Trades. *Cellular Signalling*, **26**, 2683-2693. https://doi.org/10.1016/j.cellsig.2014.08.017

[17] Wu, Z., Hundsdoerfer, P., Schulte, J.H., Astrahantseff, K., Boral, S., Schmelz, K., *et*

al. (2021) Discovery of Spatial Peptide Signatures for Neuroblastoma Risk Assessment by MALDI Mass Spectrometry Imaging. *Cancers*, **13**, Article No. 3184. https://doi.org/10.3390/cancers13133184

[18] Suh, J.M., Son, Y., Yoo, J.Y., Goh, Y., Seidah, N.G., Lee, S., *et al.* (2021) Proprotein Convertase Subtilisin/Kexin Type 9 Is Required for Ahnak-Mediated Metastasis of Melanoma into Lung Epithelial Cells. *Neoplasia*, **23**, 993-1001. https://doi.org/10.1016/j.neo.2021.07.007

[19] Prat, A., Navarro, A., Paré, L., Reguart, N., Galván, P., Pascual, T., *et al.* (2017) Immune-Related Gene Expression Profiling after PD-1 Blockade in Non-Small Cell Lung Carcinoma, Head and Neck Squamous Cell Carcinoma, and Melanoma. *Cancer Research*, **77**, 3540-3550. https://doi.org/10.1158/0008-5472.CAN-16-3556

[20] Hu, J., Yu, A., Othmane, B., Qiu, D., Li, H., Li, C., *et al.* (2021) Siglec15 Shapes a Non-Inflamed Tumor Microenvironment and Predicts the Molecular Subtype in Bladder Cancer. *Theranostics*, **11**, 3089-3108. https://doi.org/10.7150/thno.53649

[21] Belli, C., Trapani, D., Viale, G., D'Amico, P., Duso, B.A., Della Vigna, P., *et al.* (2018) Targeting the Microenvironment in Solid Tumors. *Cancer Treatment Reviews*, **65**, 22-32. https://doi.org/10.1016/j.ctrv.2018.02.004

[22] Cardoso, A.P., Pinto, M.L., Castro, F., Costa, Â.M., Marques-Magalhães, Â., Canha-Borges, A., *et al.* (2021) The Immunosuppressive and Pro-Tumor Functions of CCL18 at the Tumor Microenvironment. *Cytokine & Growth Factor Reviews*, **60**, 107-119. https://doi.org/10.1016/j.cytogfr.2021.03.005

[23] Bremnes, R.M., Busund, L.T., Kilvær, T.L., Andersen, S., Richardsen, E., Paulsen, E.E., *et al.* (2016) The Role of Tumor-Infiltrating Lymphocytes in Development, Progression, and Prognosis of Non-Small Cell Lung Cancer. *Journal of Thoracic Oncology*, **11**, 789-800. https://doi.org/10.1016/j.jtho.2016.01.015

[24] Joseph, M. and Enting, D. (2019) Immune Responses in Bladder Cancer-Role of Immune Cell Populations, Prognostic Factors and Therapeutic Implications. *Frontiers in Oncology*, **9**, Article No. 1270. https://doi.org/10.3389/fonc.2019.01270

[25] Helm, O., Held-Feindt, J., Grage-Griebenow, E., Reiling, N., Ungefroren, H., Vogel, I., *et al.* (2014) Tumor-Associated Macrophages Exhibit Pro- and Anti-Inflammatory Properties by Which They Impact on Pancreatic Tumorigenesis. *International Journal of Cancer*, **135**, 843-861. https://doi.org/10.1002/ijc.28736

[26] Jiang, P., Gu, S., Pan, D., Fu, J., Sahu, A., Hu, X., *et al.* (2018) Signatures of T Cell Dysfunction and Exclusion Predict Cancer Immunotherapy Response. *Nature Medicine*, **24**, 1550-1558. https://doi.org/10.1038/s41591-018-0136-1

[27] Wang, J., Lu, S., Yu, X., Hu, Y., Sun, Y., Wang, Z., *et al.* (2021) Tislelizumab plus Chemotherapy vs Chemotherapy Alone as First-Line Treatment for Advanced Squamous Non-Small-Cell Lung Cancer: A Phase 3 Randomized Clinical Trial. *JAMA Oncology*, **7**, 709-717. https://doi.org/10.1001/jamaoncol.2021.0366